

# Phase separation at the magnetic-superconducting transition in



**Giacomo Prando<sup>\*1</sup>, Samuele Sanna<sup>2</sup>, Gianrico Lamura<sup>3</sup>, Toni Shiroka<sup>4</sup>, Matteo Tropeano<sup>3,5</sup>, Andrea Palenzona<sup>3</sup>, Hans-Joachim Grafe<sup>1</sup>, Bernd Büchner<sup>1,6</sup>, Pietro Carretta<sup>2</sup>, Roberto De Renzi<sup>7</sup>**

<sup>1</sup> Leibniz-Institut für Festkörper- und Werkstofforschung (IFW) Dresden, D-01171 Dresden, Germany

<sup>2</sup> Dipartimento di Fisica and Unità CNISM di Pavia, Università di Pavia, I-27100 Pavia, Italy

<sup>3</sup> CNR-SPIN and Università di Genova, I-16146 Genova, Italy

<sup>4</sup> Laboratorium für Festkörperphysik, ETH-Hönggerberg, CH-8093 Zürich, Switzerland

<sup>5</sup> Columbus Superconductors S. p. A., I-16133 Genova, Italy

<sup>6</sup> Institut für Festkörperphysik, Technische Universität Dresden, D-01062 Dresden, Germany

<sup>7</sup> Dipartimento di Fisica and Unità CNISM di Parma, Università di Parma, I-43124 Parma, Italy

**Key words:** Pnictides,  $\mu^+$ SR,  $^{19}\text{F}$ -NMR, magnetism, superconductivity.

\* Corresponding author: e-mail g.prando@ifw-dresden.de, Phone: +49-351-4659-668, Fax: +49-351-4659-540

In this paper we report a detailed  $\mu^+$ SR and  $^{19}\text{F}$ -NMR study of the  $\text{La}_{0.7}\text{Y}_{0.3}\text{FeAsO}_{1-x}\text{F}_x$  class of materials. Here, the diamagnetic  $\text{La}_{1-y}\text{Y}_y$  substitution increases chemical pressure and, accordingly, sizeably enhances the optimal superconducting transition temperature. We investigate the magnetic-superconducting phase transition by keeping the Y content constant ( $y = 0.3$ ) and by varying the F content in the range  $0.025 \leq x \leq 0.15$ .

Our results show how magnetism and superconductivity coexist for  $x = 0.065$ . Such coexistence is due to segregation of the two phases in macroscopic regions, resembling what was observed in  $\text{LaFeAsO}_{1-x}\text{F}_x$  materials under applied hydrostatic pressure. This scenario is qualitatively different from the nanoscopic coexistence of the two order parameters observed when La is fully substituted by magnetic rare-earth ions like Sm or Ce.

Copyright line will be provided by the publisher

**1 Introduction** The emergence of high-temperature superconductivity nearby the disruption of a long-range magnetic state is a common feature of both the cuprates and iron-pnictide compounds, possibly hinting at a common magnetic mechanism for the Cooper pairing. In many of the latter materials, the magnetic and superconducting states are known to coexist nanoscopically [1,2,3,4,5] while in others they are reported to be macroscopically segregated [6,7]. In the  $\text{REFeAsO}_{1-x}\text{F}_x$  family with RE = La no coexistence at all has been found up to now [8], even if a macroscopic segregation was observed upon the application of hydrostatic pressure [9].

In order to better understand this phenomenology in the case of  $\text{REFeAsO}_{1-x}\text{F}_x$  (RE1111) with RE = La and to eventually compare the effect of chemical and hydrostatic pressures in such materials, we have studied the class of compounds  $\text{La}_{0.7}\text{Y}_{0.3}\text{FeAsO}_{1-x}\text{F}_x$  at different charge doping levels  $x$ . The investigated samples were loose pow-

ders prepared as reported in previous works [10,11]. Here, as an effect of the internal pressure triggered by the different ionic radii of La and Y, the diamagnetic  $\text{La}_{1-y}\text{Y}_y$  substitution enhances the superconducting transition temperature  $T_c$  from 26 K ( $y = 0$ ) to 32 K ( $y = 0.3$ ) at optimal F doping, namely  $x = 0.15$  [10]. The magnetic-superconducting transition was then investigated by tuning the F content in the range  $0.025 \leq x \leq 0.15$  and by keeping the yttrium content fixed to  $y = 0.3$ .

**2 Spin-density wave phase** Zero-magnetic field (ZF)  $\mu^+$ SR measurements were performed in order to follow the  $x$ -dependence of the magnetic volume fraction  $V_m(T)$  of the spin-density wave (SDW) phase. Experiments were carried out at the GPS facility of the  $S\mu\text{S}$  muon source at the Paul Scherrer Institut (PSI). For all the

Copyright line will be provided by the publisher

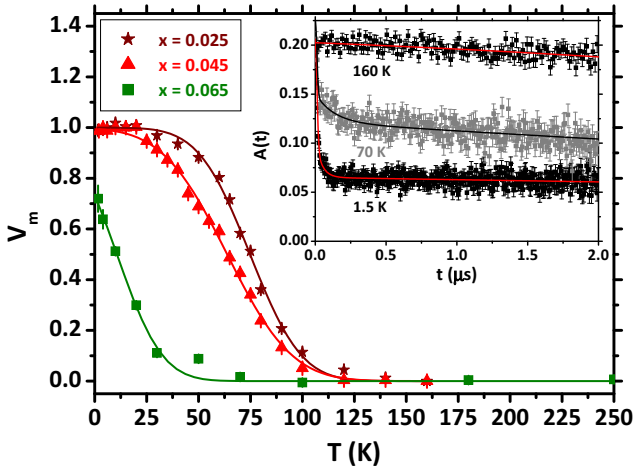


**Figure 1** Main panel: magnetic volume fraction  $V_m(T)$  for  $0.025 \leq x \leq 0.065$  after fitting experimental data by means of Eq. 1. Continuous lines are best fits to data according to erf-like functions. Inset: raw data for  $x = 0.025$  at different  $T$  values. Continuous lines are best fits to data according to Eq. 1.

investigated temperature values ( $T$ ) the general expression

$$A_T(t) = A_0 [1 - V_m(T)] e^{-\frac{\sigma^2 t^2}{2}} + A_0 [a^\perp(T)F(t)D^\perp(t) + a^\parallel(T)D^\parallel(t)] \quad (1)$$

fits the muon-spin depolarization function as a function of time ( $t$ ). In the paramagnetic limit,  $V_m(T) = 0$ , no static field of electronic origin contributes to the depolarization and only the weak contribution from the nuclear magnetic moments leads to a slow gaussian depolarization with characteristic rate  $\sigma$ . Below the magnetic-order transition temperature  $T_N$ , the superscript  $\perp$  ( $\parallel$ ) refers to the fraction of muons experiencing a local static magnetic field in a perpendicular (parallel) direction with respect to the initial muon spin polarization. Accordingly, the amplitudes  $a^{\perp,\parallel}$  must satisfy the requirement  $[a^\perp(T) + a^\parallel(T)] = V_m(T)$ . A coherent precession of the implanted muons around the local magnetic field  $B_\mu$  can then be discerned in the  $a^\perp$  amplitudes and described by the oscillating function  $F(t)$  damped by the function  $D^\perp(t) = \exp(-\lambda^\perp t)$ .

If the distribution of  $B_\mu$  values is too broad, the fast dephasing of the muon-spins' leads to an overdamping of the signal preventing one from observing any precession. This is the case for the investigated samples (see the inset of Fig. 1, relative to the case of  $x = 0.025$ ). It should be remarked that a small transverse component  $a_s^\perp$  was needed in addition to the main one,  $a_f^\perp$ . The two subscripts refer to the different extents of slow ( $\lambda_s^\perp \sim 10 \mu\text{s}^{-1}$ ) and fast ( $\lambda_f^\perp \sim 60 \mu\text{s}^{-1}$ ) transversal damping. These two components are likely to be associated with the two muon sites observed in pure  $\text{LaFeAsO}$  [12].

The comparison of  $V_m(T)$  for  $0.025 \leq x \leq 0.065$  is displayed in Fig. 1. It is clear that the effect of  $\text{O}^{2-}/\text{F}^-$

substitution is a gradual suppression of the magnetic critical temperature  $T_N$ , defined as the temperature where  $V_m(T) = 0.5$ . This strongly resembles previous reports for other RE1111 materials [4, 8]. Samples are fully magnetic at low  $T$  for  $x \leq 0.045$ . The  $x = 0.065$  compound, on the other hand, shows a magnetic volume fraction  $V_m \simeq 0.7$  at 1.5 K, namely the sample does not fully turn magnetic down to the lowest investigated temperature. Any further increase in  $x$  is then expected to completely suppress magnetism in the material.

**3 Superconducting phase** Measurements of magnetic susceptibility were used to establish the superconducting critical temperatures  $T_c$  for  $x \geq 0.065$  samples. The results of field-cooled (FC) curves at  $H = 1$  Oe are presented in Fig. 2. For the two investigated samples belonging to this doping region one finds  $T_c(x = 0.065) = 26.5 \pm 0.5$  K and  $T_c(x = 0.15) = 32.0 \pm 0.5$  K. By extrapolating the magnetization values at zero  $T$ , it is possible to compare the relative shielding fractions for the samples from the ratio  $M(0)_{x=0.065}/M(0)_{x=0.15} \sim 0.35$ .

A more precise estimate of the absolute values of the shielding fractions for the two samples is possible by considering the results of the transverse-field (TF)  $\mu^+$ SR experiments performed on the  $x = 0.15$  sample at ISIS (Rutherford-Appleton Laboratories, UK) in the MuSR spectrometer (raw data not shown). In this experiment a magnetic field  $|\mathbf{H}_{\text{ext}}| = 150$  Oe is applied to the sample in a direction perpendicular to the initial spin polarization of the implanted muons. For  $T \gg T_c$  the sample is in a fully-paramagnetic regime and all the muons precess coherently around  $\mathbf{H}_{\text{ext}}$ . No damping of the coherent precession is active, with the only exceptions of the weak one associated

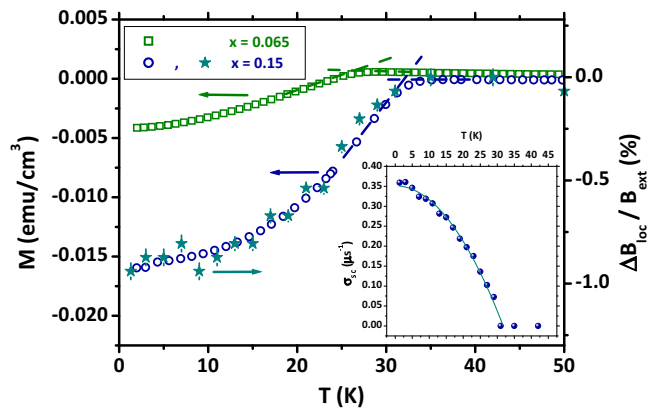


**Figure 2** Main panel: FC magnetization of the two samples  $x = 0.065$  and  $x = 0.15$  at  $H = 1$  Oe (open symbols). Intercepts of the dashed lines allow the estimate of  $T_c$ . Blue stars quantify the diamagnetic screening probed by muons in  $x = 0.15$  (see text). Inset:  $T$ -dependence of the damping  $\sigma_{\text{SC}}$  of the TF- $\mu^+$ SR signal introduced by the penetration of vortex lines into the  $x = 0.15$  sample (see text). The continuous line is a best fit to data according to Eq. 3.

to the nuclear magnetism, quantified by  $\sigma$  as in Eq. 1, and of the possible contribution from diluted magnetic impurities, causing an exponential damping quantified by  $\lambda_{\text{imp}}$ . On the other hand, a lattice of vortex lines is expected to be present inside the sample for  $T < T_c$ . This, in turn, gives rise to a modulation of the spatial profile of  $H_{\text{ext}}$  resulting in a Gaussian extra-damping of the muon precession frequency [13] quantified by  $\sigma_{\text{SC}}$  in the fitting function

$$A_T(t) = A_0 \cos(\gamma B_\mu t) e^{-\frac{(\sigma_{\text{SC}}^2 + \sigma^2)t^2}{2}} e^{-\lambda_{\text{imp}} t}. \quad (2)$$

At the same time, the shielding of  $H_{\text{ext}}$  by the superconducting phase leads to a sizeable lowering of the internal field  $B_\mu$  felt by the muons. This diamagnetic shielding is typically quantified by the quantity  $\Delta B_{\text{loc}} \equiv B_\mu - H_{\text{ext}}$ .

By fitting the experimental data above  $T_c$  according to Eq. 2, one can find that the value of  $\lambda_{\text{imp}}$  is almost constant at  $\sim 0.18 \mu\text{s}^{-1}$  for  $T_c \leq T \leq 100$  K. This allows us to keep  $\lambda_{\text{imp}}$  as a fixed parameter also for  $T \leq T_c$  incorporating all the extra-broadening of the line in  $\sigma_{\text{SC}}$ . Fitting results are presented in Fig. 2. The  $\sigma_{\text{SC}}$  vs  $T$  trend is well described by the function

$$\sigma_{\text{SC}} = \sigma_{\text{SC}}(0) \left[ 1 - \left( \frac{T}{T_c} \right)^2 \right] \quad (3)$$

as previously reported for  $\text{LaFeAsO}_{1-x}\text{F}_x$  [13]. The saturation value  $\sigma_{\text{SC}}(0) = 0.350 \pm 0.005 \mu\text{s}^{-1}$  allows us to deduce an in-plane penetration depth  $\lambda_{\text{ab}}(0) = 420 \pm 10$  nm at zero  $T$  (see Ref. [5] for details).

From the observation that all the muons feel a static field lower than  $H_{\text{ext}}$  (Fig. 2) we conclude that superconductivity in the  $x = 0.15$  compound is a bulk phenomenon extended over the whole sample volume. Similarly, magnetization data and TF- $\mu^+$ SR measurements imply a superconducting volume fraction of only  $\sim 35\%$  for the  $x = 0.065$  compound. Considering that the magnetic volume fraction at  $T = 0$  K is  $\sim 70\%$  we argue that in this sample magnetism and superconductivity are macroscopically separated. A similar scenario has been derived in  $\text{LaFeAsO}_{1-x}\text{F}_x$ , where the ratio of the superconducting and the magnetic volume fractions was tuned by the application of external hydrostatic pressure [9].

**4 Low-energy spin dynamics** Further insights were obtained by means of  $^{19}\text{F}$ -NMR measurements on the samples  $0.045 \leq x \leq 0.15$ . Here, the main quantity of interest is the so-called spin-lattice relaxation time  $T_1$  for the  $^{19}\text{F}$  ( $I = 1/2$ ) nuclear spins, quantifying the time required by the nuclear magnetization  $M$  to relax back to the thermodynamical equilibrium along the quantization axis, once a proper radio-frequency pulse sequence has brought the system into a saturation condition [14]. A conventional sequence  $(\pi/2)_{\text{sat}} - t - (\pi/2) - \tau_{\text{echo}} - (\pi/2)$  was employed

to this aim. The quantity

$$y(t) = 1 - \frac{M(t)}{M(\infty)} = \exp \left[ - \left( \frac{t}{T_1} \right)^\beta \right] \quad (4)$$

could then be measured, where the stretching parameter  $\beta$  accounts for a distribution of relaxation times (raw data are reported in the inset of Fig. 3). When considering relaxation processes involving nuclear spins with  $I = 1/2$ , values  $\beta < 1$  typically imply indeed an inhomogeneity of the local environment of the nuclei. Typical measured values are  $\beta \sim 0.6$  for  $x = 0.045$  and  $x = 0.065$  while  $\beta \sim 0.85$  for  $x = 0.15$ . The interplay between  $\text{La}_{1-y}\text{Y}_y$  and  $\text{O}_{1-x}\text{F}_x$  dilutions is likely to be the main source of such disorder in the examined compounds.

The relaxation rate  $1/T_1$  as a function of  $T$  is reported in the main panel of Fig. 3 for the samples  $x = 0.045$ ,  $x = 0.065$  and  $x = 0.15$ . By keeping into account the common occurrence of power-law functional forms for  $1/T_1$  in RE1111 materials [15,16], data relative to the fully magnetic sample  $x = 0.045$  can be properly described by the following relation

$$\frac{1}{T_1} = \left( \frac{1}{T_1} \right)_{\text{FL}} + \left( \frac{1}{T_1} \right)_{\text{SF}} = K_{\text{FL}} T + K_{\text{SF}} T^{-2}. \quad (5)$$

where the exponent in the SF contribution should be considered as a phenomenological parameter. The term FL accounts for relaxation processes driven by conduction electrons belonging to a Fermi liquid and resulting in a

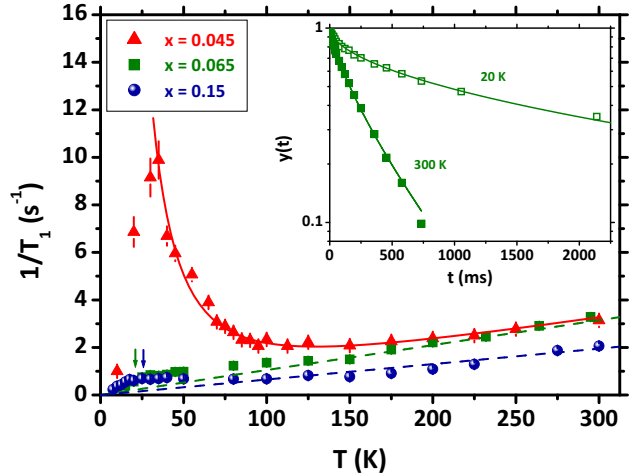


**Figure 3** Main panel:  $1/T_1$  vs  $T$  of  $^{19}\text{F}$  nuclei for the investigated samples. The continuous line is a best fit to data according to Eq. 5. Dashed lines are linear best fit to data accounting for Korringa-like relaxation. Arrows indicate the onset of superconductivity for  $x = 0.065$  and  $x = 0.15$ . Inset:  $y(t)$  at different  $T$  for  $x = 0.065$ . Continuous lines are best fits to data according to Eq. 4. Measurements have been performed at  $H_0 = 39$  KOe.

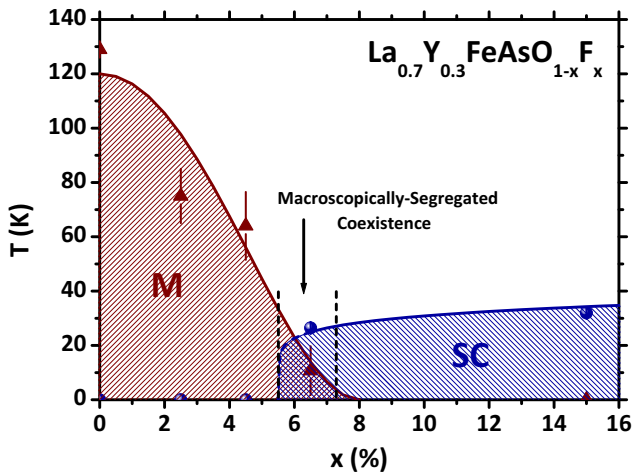


**Figure 4** Phase diagram for the electronic ground states of  $\text{La}_{0.7}\text{Y}_{0.3}\text{FeAsO}_{1-x}\text{F}_x$  materials as a function of  $x$  as obtained by combining  $\mu^+\text{SR}$  and SQUID data. The  $T_N$  value for  $x = 0$  is taken from resistivity measurements reported in Ref. [11].

linear  $T$ -dependence (so-called Korringa-like relaxation) [14]. As a result of the fitting procedure,  $K_{\text{FL}} = 0.011 \pm 0.001 \text{ s}^{-1}\text{K}^{-1}$ . The term SF in Eq. 5 can be associated to spin fluctuations arising from the gradual magnetic correlations eventually leading to the SDW phase at low  $T$ .

For the two superconducting samples the term FL is the leading relaxation channel besides small upturns with decreasing  $T$  towards  $T_c$ . Fitting leads to  $K_{\text{FL}} = 0.011 \pm 0.001 \text{ s}^{-1}\text{K}^{-1}$  and  $K_{\text{FL}} = 0.006 \pm 0.001 \text{ s}^{-1}\text{K}^{-1}$  for  $x = 0.065$  and  $x = 0.15$ , respectively, suggesting a gradual suppression of the density of states at the Fermi energy. With further decreasing of  $T$  below  $T_c$ , the relaxation rate in both samples decreases much more steeply. This result again confirms that  $^{19}\text{F}$  nuclei are sensitive to processes involving bands from the FeAs layers.

**5 Phase diagram and conclusions** The phase diagram in Fig. 4 displays the magnetic and superconducting transition temperatures as a function of  $x$  for the  $\text{La}_{0.7}\text{Y}_{0.3}\text{FeAsO}_{1-x}\text{F}_x$  samples under investigation.

The main effect of F doping is the progressive suppression of magnetism and the appearance of superconductivity, resembling the general behavior of the RE1111 family. It is important to stress that here the samples display macroscopic phase separation at the magnetic-superconducting boundary. To the best of our knowledge, this behavior has never been observed before for the RE1111 compounds at ambient pressure. Instead, materials with RE = La display a sharp first-order-like magnetic-superconducting transition and no coexistence has been reported up to now [8]. However, macroscopic phase separation of magnetic and superconducting volumes can be induced by applying hydrostatic pressure to

non-superconducting La1111 samples with F content close to the disruption of magnetism [9]. By considering that a similar macroscopic phase separation is here reported for  $\text{La}_{0.7}\text{Y}_{0.3}\text{FeAsO}_{1-x}\text{F}_x$  samples, we can conclude that the chemical pressure produced by the partial Y substitution of La mimics closely the effect of the hydrostatic pressure.

## References

- [1] S. Sanna, R. De Renzi, T. Shiroka, G. Lamura, G. Prando, P. Carretta, M. Putti, A. Martinelli, M. R. Cimberle, M. Tropeano, and A. Palenzona, *Phys. Rev. B* **82**, 060508(R) (2010).
- [2] S. Sanna, P. Carretta, P. Bonfá, G. Prando, G. Allodi, R. De Renzi, T. Shiroka, G. Lamura, A. Martinelli, and M. Putti, *Phys. Rev. Lett.* **107**, 227003 (2011).
- [3] E. Wiesenmayer, H. Luetkens, G. Pascua, R. Khasanov, A. Amato, H. Potts, B. Banusch, H.-H. Klauss, and D. Johrendt, *Phys. Rev. Lett.* **107**, 237001 (2011).
- [4] T. Shiroka, G. Lamura, S. Sanna, G. Prando, R. De Renzi, M. Tropeano, M. R. Cimberle, A. Martinelli, C. Bernini, A. Palenzona, R. Fittipaldi, A. Vecchione, P. Carretta, A. S. Siri, C. Ferdeghini, and M. Putti, *Phys. Rev. B* **84**, 195123 (2011).
- [5] Z. Shermadini, H. Luetkens, R. Khasanov, A. Krzton-Maziopa, K. Conder, E. Pomjakushina, H.-H. Klauss, and A. Amato, *Phys. Rev. B* **85**, 100501(R) (2012).
- [6] M.-H. Julien, H. Mayaffre, M. Horvatić, C. Berthier, X. D. Zhang, W. Wu, G. F. Chen, N. L. Wang and J. L. Luo, *Europhys. Lett.* **87**, 37001 (2009).
- [7] Y. Texier, J. Deisenhofer, V. Tsurkan, A. Loidl, D. S. Inosov, G. Friemel, and J. Bobroff, *Phys. Rev. Lett.* **108**, 237002 (2012).
- [8] H. Luetkens, H.-H. Klauss, M. Kraken, F. J. Litterst, T. Dellmann, R. Klingeler, C. Hess, R. Khasanov, A. Amato, C. Baines, M. Kosmala, O. J. Schumann, M. Braden, J. Hamann-Borrero, N. Leps, A. Kondrat, G. Behr, J. Werner, and B. Büchner, *Nature Mater.* **8**, 305 (2009).
- [9] R. Khasanov, S. Sanna, G. Prando, Z. Shermadini, M. Bendele, A. Amato, P. Carretta, R. De Renzi, J. Karpinski, S. Katrych, H. Luetkens, and N. D. Zhigadlo, *Phys. Rev. B* **84**, 100501(R) (2011).
- [10] M. Tropeano, C. Fanciulli, F. Canepa, M. R. Cimberle, C. Ferdeghini, G. Lamura, A. Martinelli, M. Putti, M. Vignolo, and A. Palenzona, *Phys. Rev. B* **79**, 174523 (2009).
- [11] A. Martinelli, A. Palenzona, M. Tropeano, C. Ferdeghini, M. R. Cimberle, and C. Ritter, *Phys. Rev. B* **80**, 214106 (2009).
- [12] R. De Renzi, P. Bonfá, M. Mazzani, S. Sanna, G. Prando, P. Carretta, R. Khasanov, A. Amato, H. Luetkens, M. Bendele, F. Bernardini, S. Massida, A. Palenzona, M. Tropeano, and M. Vignolo, *Supercond. Sci. Technol.* **25**, 084009 (2012).
- [13] H. Luetkens, H.-H. Klauss, R. Khasanov, A. Amato, R. Klingeler, I. Hellmann, N. Leps, A. Kondrat, C. Hess, A. Köhler, G. Behr, J. Werner, and B. Büchner, *Phys. Rev. Lett.* **101**, 097009 (2008).
- [14] C. P. Slichter, *Principles of Magnetic Resonance*, Springer-Verlag Berlin (1990)
- [15] E. M. Brüning, C. Krellner, M. Baenitz, A. Jesche, F. Steglich, and C. Geibel, *Phys. Rev. Lett.* **101**, 117206 (2008).

- [16] G. Prando, P. Carretta, A. Rigamonti, S. Sanna, A. Palenzona, M. Putti, and M. Tropeano, *Phys. Rev. B* **81**, 100508(R) (2010).